UNSYS digital

Journal of Unmanned System Technology

Navigation of an ROV by Non-Hybrid Cable Using FAMPLC Technique

Alireza Nazem, Mohd Rizal Arshad

School of Electrical and Electronic Engineering, Universiti Sains Malaysia
Pinang, Malaysia

***Abstract*—** Non-hybrid cable for underwater application is a downgraded cable since there is no fibre layer in the shield. The optical communication technique in underwater applications necessitates the need of multi plies of the fibre layers that result in a massive cable size, serious maintenance and high cost. The novel technique of FAMPLC introduces a combined large signal modulation of the supplying voltage frequency and the consumer current amplitude over the entire power line. This technique requires a server inclusive of an embedded DC to AC bridge inverter in one end and a dummy load used for current modulation in another end. The transmitted data are extracted from the frequency and the duty cycle of the pulse trains. The technique allows real time full-duplex power-line communication. The wait-state and handshaking sequences between send and receive intervals are also eliminated in this technique. Nevertheless, user needs to define a lookup Table for desired commands and data processing. In this paper the noise handling and a self-calibration method is also discussed.

***Keywords*—** FAMPLC, non-hybrid cable, voltage frequency modulation, current amplitude modulation, power-line communication.

I. INTRODUCTION

The conventional communication technique in underwater industry applications utilizes the optical platform in a hybrid cable for the long distant data and signal transmissions. Although the stability and noise, as the main considerable factors in this method are respectively high and low, there are inherent drawbacks that encourage further studies for improvements or replacement techniques as well. Many users are unanimous about the two factors of material and maintenance costs which are fairly high in this technique [1]. More information about the conventional optical method can be found in [2] and [3]. FAMPLC can be integrated within an independent power source for any remotely controlled application. This technique is introduced as a robust and reliable substitution for the optical transmission method. Apart from the fibre base communication method, in other conventional data transmission techniques using copper layers, such as the Supervisory Control And Data Acquisition (SCADA) system, that is interfaced between the sensors and devices and the Programmable Logic Controllers (PLCs) [4], a dedicated power cable in addition to the data line is also required to power up the SCADA system. In 2009, Industrial Power-line Communication (IPLC) was also presented [5]. In this technique, the power cables of the DC link are used as transmission medium and thus do not require any other cable. This is achieved by a coupling unit that couples the data onto the power cables, thus reduces the cabling effort considerably. In comparison with other power-line communication methods such as the Frequency Shift Keying (FSK), the maximum copper length is considered for couples of hundred meters (<1000m). FSK is a robust modulation technique which is virtually unaffected by unpredictable attenuation and phase distortion in the power-line channel [6]. In medium voltage power system, multiple repeaters with dedicated IDs are required to compensate the signal drop due to the distance [7].

Using FAMPLC as a large signal power line carrier, a DC to low frequency AC H-bridge inverter is used to generate a Frequency Modulation (FM) over the converted AC power. The linear characteristics of a multiply conductor cable in low frequencies (<1KHz) allows longer distance data transmission [8]. The source, named as FAM server, is located in the controller cabin. It transmits the data to the receiver using the parameters of the frequency that affects both the frequency and the duty cycle of the supplying power. Thus, both the pulse-width and the frequency; carry the value based on the predefined lookup Table. The receiver will recognize the values based on every respected frequency and duty cycle. For data transmission from the receiver, an amplitude modulation is generated over the draining current using an active resistance as a dummy load. The effect of the overlaid current is sensible by an embedded detector in the server. A Thevenin Equivalent Converter (TEC) circuit is deployed in the server to leverage the voltage means from the draining current. **Figure 1** illustrates the exaggerated effect of frequency and amplitude combined modulations over the power-line observed from the ROV side.

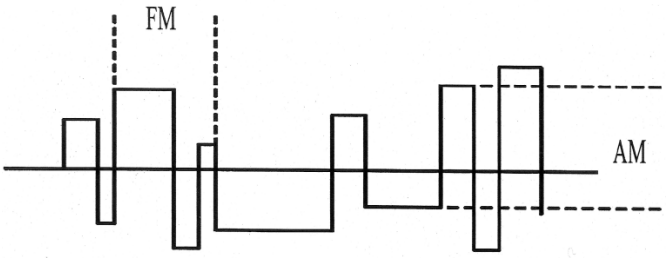

Figure 1 The effect of the frequency and amplitude combined modulations observed from the ROV side

Corresponding author: Mohd Rizal Arshad (e-mail: rizal@eng.usm.my)

This paper was submitted on July 09, 2013; revised on August 6, 2013; and accepted on September 6, 2013.

The next process is to read the widths of the receiving pulse and period for extraction of the frequency (*f*) and the duty cycle (*D*). In order to communicate using amplitude modulation over the power-line, there will be more sequential processes compared to frequency modulation mode from the server to the receiver. **Figure 2** shows the comparison of computing processes in an individual transmission format. The value of the frequency and the duty cycle of receiving signal are compared with a predefined lookup Table for all desired functions.

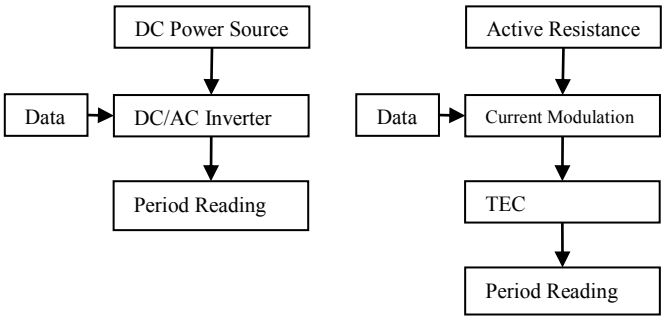

Figure 2 The comparison of computing processes: a. FM, b. AM

Thevenin equivalent impedance will be the inner impedance of the whole electric network. Both Thevenin equivalent parameters and load impedance won't be constant and will depend on the network topology structure, system operation pattern, generation status and reactive power sources [9].

Hybrid cables in distant underwater applications have typically the buoyant feature as one of their inherent factor. According to our recent investigation, the non-hybrid copper base buoyant cable for ROVs has yet to be commercialized for the FAMPLC technique probably due to market's unwillingness to use power line solution for the ROV application so far.

II. Approach and Methods

A. Server's Transmitter

The fundamental concept of the FAM communication from the server is based on an electronically inverted AC power in which the frequency information is utilized to transmit data. Although data is extracted from the period of the AC power at the receiver point, the waveform has a *specifying effect* in the reading process from the receiver back to the server. Meaning that, in the server transmitting point, any kind of periodic waveform may carry the means of data to the ROV, but the reliability of the transmission from the ROV to the server varies depends on the incoming waveform. For instance, a generated sine wave by the server may result in losses of receiving data from the ROV to the server within the intervals closed to 0, π and 2π while square wave results in a fewer disturbing phenomenon in these points [10]. The fundamental components of the system circuitry are shown in **Figure 3**. Both kinds of alternative or direct current may be considered for the server power as the source for the bridge switches. Data will be the value carried by the switch drivers which control the frequency and the duty cycle.

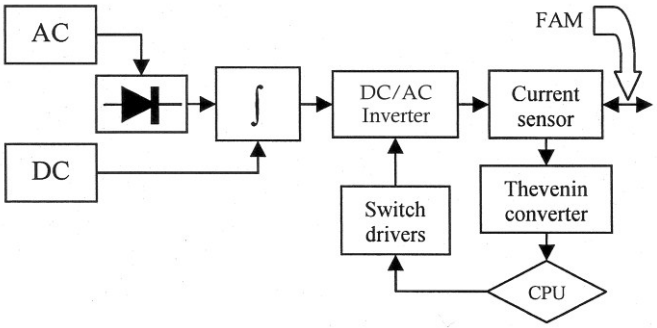

Figure 3 The fundamental components of FAM architecture

The data extraction from the power components in FAMPLC is based on a counting process. Every voltage or current pulse triggers two embedded counters by its rising edge. Hence, the consequent falling and rising edges will stop the counters respectively. Whereby, the value of the first interval belongs to the duty cycle of the pulse, and the second one presents its frequency. These values are predefined in a lookup table for the required command and data means.

B. Client's Transmitter

As discussed before, an active resistance as a dummy load such as shown in **Figure 4** is employed to generate variation of current drain. Norton's equivalent circuit for this configuration may also be considered. It is being controlled to modulate the data over the current. The transmitted data can be in both analog and digital forms. *Q* may be chosen from the medium power range of unipolar or bipolar (Junction) transistors.

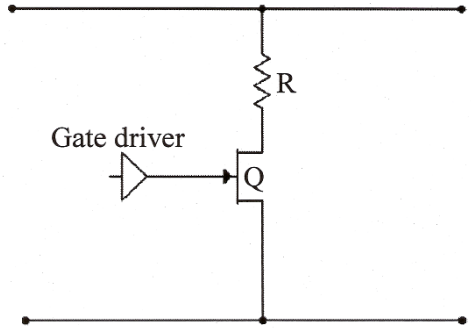

Figure 4 The active resistance model used for the current modulation

C. Equivalent Transmission Circuit

The effect of inductance and the capacitance vectors on transmitting signal in low frequencies (<100Hz) could be negligible in an ideal model. Whereas, the dynamic characteristics are equal, thus results in a resistive model. However, this ideal condition is almost out of reach due to the manufacturing parameters. On the other hand, since the cable uses a parallel form of copper pair, the current vectors in each copper ply oppose one another in an umbilical form. Thus, the loss due to Electromagnetic Force (EMF) inclines to zero and produces a negligible impulsive force [11]. A combination of two elementary cells for bidirectional transmission line results in an equivalent circuit of the cable characteristics [12]. **Figure 5** illustrates a base frequency cable model which is considerable

for FAM [13]. $Z_c^{'}$ presents the equivalent inductive dual model for the cable's capacitance.

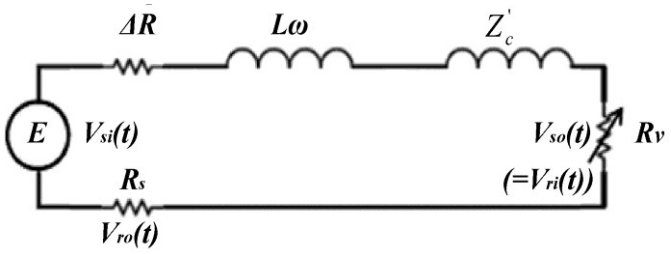

Figure 5 Equivalent circuit for a pair of copper wire

D. Server's Transfer Function

Since *Rs* is a very low ohm resistor (typically < 0.1Ω) just for the sake of current sampling, thus the voltage drop due to it can be assumed negligible in large scale calculations. So that the server's transfer function $H_v(f)$ for the linear time invariant concept [14-15-16] for this model can be obtained as in (**1**):

$$H_V(f) = \frac{V_{so}(t)}{V_{si}(t)} \tag{1}$$

or

$$H_V(f) = \frac{R_V}{\Delta R} + \Delta L \cdot \omega + Z_c' \tag{2}$$

It is obvious that the increase of the frequency results in more copper loss and the phase of the frequency as shown in the **Figure 6**, will be also underdamped and shifted.

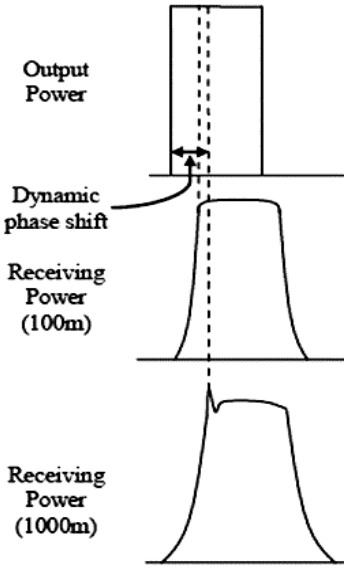

Figure 6 Shifting phenomena of the inverted power pulse in different cable length

However, the period of the frequency which carries the means of transmitted data will not change.

E. Receiver's Transfer Function

Although $V_{ro}(t)$ is small value and requires an amplification stage, to study the effect of the signal transmission from the ROV, it may contribute directly in (**3**).

$$H_R(t) = \frac{V_{ro}(t)}{V_{ri}(t)} \tag{3}$$

Knowing that

$$V_{ro}(t) = R_S \cdot i_S \tag{4}$$

Using the Kirchoff's law

$$V_{ro}(t) = E - i_2 \cdot \Delta R - L_L \cdot \frac{di_2}{dt} - L_C \cdot \frac{di_2}{dt} - i_2 \cdot R_V \tag{5}$$

Thus the transfer function can be expressed as in Eq. (6)

$$H_R(t) = \frac{r_E - \Delta R}{R_V} - \frac{\Delta L}{i_2 \cdot R_V} \cdot \frac{di_2}{dt} - 1 \tag{6}$$

where r_E indicates the inverter's internal resistivity inclusive of the MOSFETs' substrate resistors and *L**C*** presents the inductance value of $Z_c^{'}$. **Equation** (**7**) specifies the requirement for a stable transmission for this model. Whereas, *VR* is the voltage drops due to the resistances of the cable, *VA* is the active load and *VZ* presents the dynamic voltage drop due to the cable's impedance.

$$E - V_R > V_A - V_Z \tag{7}$$

Therefore, increase in three fundamental factors, i.e. the cable's resistivity, reactive parameters and frequency, will result in an unstable transmission. In the conditions where the voltage drop across the cable is high, the increase of the supplying voltage can compensate and reaffix the stability.

F. The Noise Handling

One of the advantages of using FAMPLC technique is its large signal feature that minimizes the effect of noise and thus, is suitable for distant remote applications. Nonetheless, the studies of the cable dynamics show that the natural behavior of the transmission layers is diametrically manageable. **Figure 7** shows an underdamped condition of a test pulse train in both the FM and AM modes. Since the measurements of the pulse widths are based on a counting process, the phase shifting effect is not accountable in our calculation. However, the rising and falling delays due to the dynamic influences have to be addressed. Considering the low-pass feature of a conventional copper cable, an exhaustive analysis using a Π model transmission line as shown in **Figure 8** yielded to obtain general expressions for each transmission mode. **Equation** (**8**) and (**9**):

$$i_S = \frac{L \cdot C}{2} \cdot \frac{d^2 i_v}{dt^2} + \frac{r_L \cdot C}{2} \cdot \frac{di_v}{dt} + i_{R_n'} + i_{AM} \tag{8}$$

The first and second terms in (**8**) present the distortion interval of the AM transmission. $i_{R_n'}$ is the system draining current, and i_{AM} is the active resistance (dummy load) current. i_{AM} is used to carry the data means over AM. The distortion analysis for transmission model shown in **Figure 8(b)** for an FM transmission can be expressed as in (**9**).

$$V_{C_2}(t) = \frac{1}{C \cdot \omega_0^2}(S_2 \cdot K_1 \cdot e^{s_1 \cdot t} + S_1 \cdot K_2 \cdot e^{s_2 \cdot t}) \tag{9}$$

Where

$$s_1 = -(\zeta_s \cdot \omega_0 - \omega_0 \cdot \sqrt{\zeta_s^2 - 1}) \tag{10}$$

$$s_2 = -(\zeta_s \cdot \omega_0 + \omega_0 \cdot \sqrt{\zeta_s^2 - 1}) \quad (10)$$

and

$$\zeta_s = \frac{r_L}{2} \cdot \sqrt{\frac{C}{L}} \quad (11)$$

is called the exponential damping ratio for the server's transmission line. K_1 and K_2 are achievable from two equations of the initial conditions of $i_C(0)$ and its time base derivative. The Total Harmonic Distortion (THD) [17] in higher frequencies depends on the dynamic characteristics of the transmission layer.

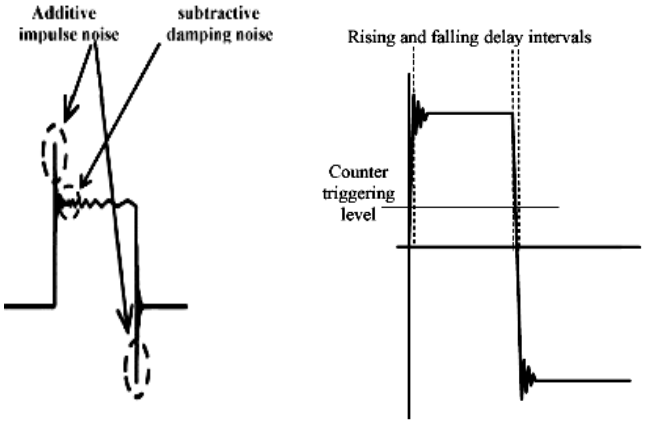

Figure 7 The received pulse in: a. The AM mode (left), b. The FM mode (right)

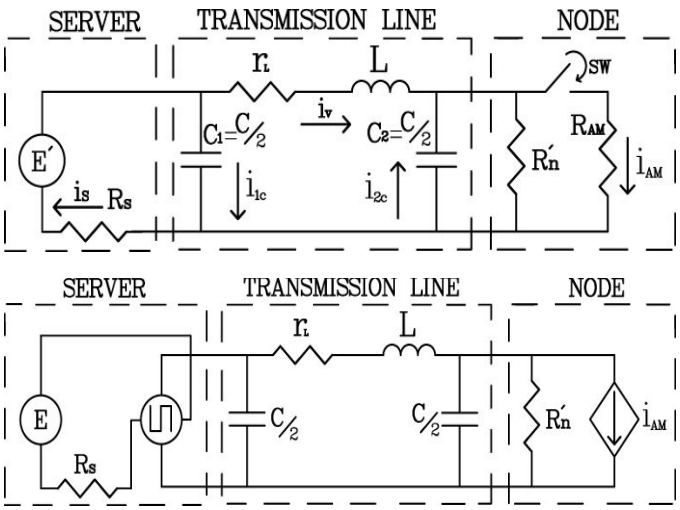

Figure 8 The Π model transmission line used for a. The AM pulse edge analysis, b. The FM pulse edge analysis

III. Results And Discussions

In a specific condition, let's consider the maximum frequency of 100Hz that causes 1.2 millisecond delays due to the phase shift phenomenon. By using AWG16 wire for 1000 meters of power cable, 2000 meter length of the copper is used. The total resistive value will be 26 ohms due to the 0.013 ohm per meter resistance value. An LCR meter used to measure the inductance and capacitance of the wire for 100 meters in the straight form. The value registered as 9μH for single ply leads to *L=180 μH* for 2000 meters for the total length. The capacitance value in 100 meters parallel pair is equal to 80nF which leads to 800nF for 1000 meters of copper pair. The values of the model factors are as below:

- $R = 26\ \Omega$
- $L = 180\ \mu H$
- $C = 800\ nF$

Z_c' is the result of a complex calculations [18] which result in (**12**).

$$Z_c' = P \cdot \omega^3 + Q \cdot \omega^2 + S \cdot \omega \quad (12)$$

where

$$P = L^2 \cdot \frac{C}{4} = 6.4 \cdot 10^{-15} \quad (13)$$

and

$$Q = L \cdot C \cdot \frac{\left(\frac{R}{2} + R_V\right)}{2} \quad (14)$$

and

$$S = R \cdot C \cdot \frac{\left(\frac{R}{2} + R_V\right)}{2} \quad (15)$$

R_V is typically set for a range of 10 to 30 ohms. The value of P shows that the third degree element in (**12**) for the maximum considered frequency (100 Hz) is fairly negligible. **Figure 9** illustrates the effect of Z_c' as a function of Rv and ω. It is obvious that the power drop due to Z_c' as a factor of a low-pass filter has a greater effect in higher resistivity of the active load, Rv. However, the lower values will cause a large voltage drop across the load and also generate bulks of heat. The optimum range for the active resistance must be set depends on the wire gauge, receiver's consumption and the length of the wire.

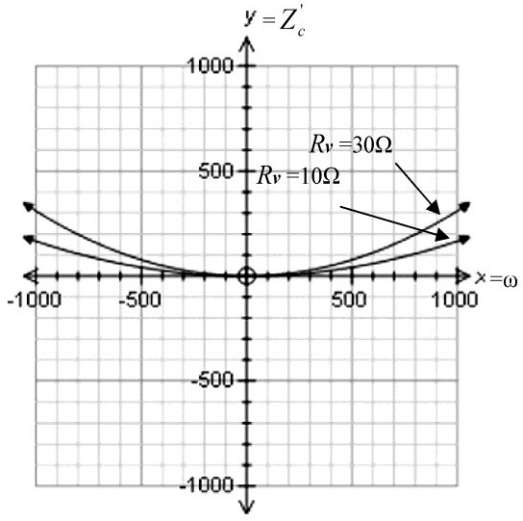

Figure 9 Line impedance as the function of ω and *Rv*

According to the result of **Figure 9**, the line impedance as the function of R_V inclines to zero for ω <300.

A. Communication Protocol

As discussed earlier a comparison process is made between a predefined lookup table and the received values at both sides. In the current research, a method in which the pulse edge triggers an incremental counting process is considered. The pulse-width is determined based on the embedded counter value. The frequency and the duty cycle are evaluated as the commander or data codes. Furthermore, a comparison is performed between the tabulated values and the counter's determination.

B. Lookup Table

Some predefined values are tabulated in **Table 1**. At the server side, output pulses from the TEC block trigger an incremental 16-bit counter for the computation of the received "*d"* values. This is an embedded counter in a medium range microcontroller unit with 16:1 counter clock ratio. Counting process starts at every rising edge and stops at the consequent falling. The first step is to categorize the result of every count. If *d* fits within any range of the "predefined" column of the **Table 1**, it is, then considered for that particular category. The second step is to convert *d* to the appropriate parametric unit related to its category. For example, if the range of -30 C° to +70 C° is considered for the temperature in the **Table 1**, *d* = 2185 results in the system temperature at 55 degrees Celsius.

Table 1 Pulsewidth values of embedded counter

Information	Predefined	*(d)*	Parametric value
Depth	1900-2000	1947	47 m
Temperature (system)	2100-2200	2185	55 C°
Temperature (environment)	2300-2400	2359	29 C°
Altimeter	2500-2600	2581	84 m
Pressure	2700-2800	2705	5 bar
Compass	2900-3260	3138	238° (from the North)

The stated values are extracted from the positive cycle of every pulse. In order to prevent any overlapping occurrence it is advisable to consider counts on ignored range between categories. In this example, the informative ranges have a gap of 100 counts from each other. Nevertheless, other methods to format and analyze the data as well as pulse-width reading, asynchronous serial transmission and superimposed analog modulation may be considered. In the given example of **Table 1**, the integer numeric system is discussed.

However, for the higher parametric accuracy, it is necessary to increase the counting speed by decreasing the ratio of the counter clock. For every one floating point digit of precision, there are three practical methods as listed below. The following suggested methods can be performed either individual or all in combination:

- The counter clock ratio is decreased
- The Microcontroller's clock is increased
- The predefined numbers are set to a wider range. In this case for a 16-bit counter maximum considerable value is 65535. A 32-bits counter may be considered for higher accuracies.

Table 2 Navigational commands

Command	Dedicated Frequency	Dedicated duty cycle	$C_P(F)$	$C_P(d)$
Stop	30 Hz	20%	16666	3333
Forward	35 Hz	30%	14285	4285
Backward	35 Hz	70%	14285	10000
Spin left	40 Hz	30%	12500	3750
Spin right	40 Hz	70%	12500	8750
Shift left	45 Hz	30%	11111	3333
Shift right	45 Hz	70%	11111	7778
Upward	50 Hz	30%	10000	3000
Downward	50 Hz	70%	10000	7000

In **Table 2** some of the navigational commands are also tabulated as an example of predefined ROV operation. Note that C_P represents the counted values for the frequency and the duty cycle.

C. Calibration

To resolve the error issues due to the dynamic effects that may cause over or undercounts, a calibrating pulse accompanies every command or data pulse ahead. This pulse is a constant value to evaluate the amount of variations. For example, let's consider that a definite voltage pulse with 10 ms width accompanies every command pulse in advance. Assuming that the clock frequency of the counter is at 500 KHz, $C_P = 5000$ will be the expected receiving value by the other party. In an occasion where the pulse edges are over-damped, the influence of the phenomenon will cause the C_P to vary. For instance, if $C_P = 4983$ is counted in this condition, the CPU will store $C_{cal} = 17$ as the calibrating value. Hence, the upcoming pulse width will be measured by considering the C_{cal}.

Table 3 Economical Comparison of hybrid and copper cables

Required cable (100 meters)	Hybrid	Copper
Cost (RM)	>2000	<1000
Winch radius (cm)	>40	<30
Weight (Kg)	>30	<20

IV. Conclusion

The current technique is introduced for elimination of the fibre base optical transmission. The technique provides a reliable and robust transmission platform for an ROV. The introduced communication model eliminates the need of sequential signal conversion by multiple transducers in optical method. Aside from this technical advantage, it is also known as a standalone (PC-less) communication platform. In addition, another benefit of the technique is presented in which the maintenance and total cost of the system is considerably reduced. In **Table 3** some economical comparison of the technique and the conventional optical method is given.

Acknowledgment

Thanks to the Universiti Sains Malaysia for facilitating this research by the PRGS grant scheme (PRGS No. 6740003)

which helped to motivate the approach for the research's outcomes.

REFERENCES

[1] L Brun, "ROV/AUV trends market and technology," *Duke University Center on Globalization, Governance & Competitiveness*, Sep. 2012, pp. 48-51.

[2] M. R. Hedayati, "ROV based acoustic emission condition monitoring & NDT of subsea fibre optic network components," in *proceeding of Suboptic 2010 conference & convention*, 2010.

[3] D. Jenkins, S. Thumbeck, "Utilizing Pressure Balanced Oil Filled (PBOF) Hose Cable Assemblies with Electric and Fibre Optic Connectors," *LLC Oceans, Technical Program*, 2008.

[4] R Kirubashankar, K Krishnamurthy & J Indra, "Remote monitoring system for distributed control of industrial plant process," *Journal of Scientific and Industrial Research*, Vol. 68, Oct. 2009, pp. 858-860.

[5] Alexander V, Stefan S, Dongsheng Y & Karl-Heinz W., "Industrial powerline communication for machine tools and robotics," *German academic society for production engineering*, Feb. 2010, pp. 295-305.

[6] Rakesh Chandra Prajapati, "Noise measurement in low-voltage Powerline for modem design and Serial data acquisition", in *proceeding of International Confrence on Information and Communication Technology,* 2007. pp.113-116.

[7] A Study on the Composite Power Line Communication Network, Duckhwa H, Younghun L & Youngdeuk M,Berlin Heidelberg, Springer-Verlag, 2009, pp. 547-554.

[8] M. Hasheminezhad, M. Vakiliant, T.R. Blackburn, & B.T. Phung, "Direct Introduction of Semicon Layers in XLPE Cable Model", in *proceeding of International Conference on Power System Technology,* 2006. pp. 1-7.

[9] Tianyu An, "Research on Illed-Conditioned Equations in Tracking Thevenin Equivalent Parameters with Local Measurements," in *proceeding of International Conference on Power System Technology,* 2006. pp. 1-4.

[10] Palash K & Arabinda D, "Microprocessor-based system for identification of phase sequence and detection of phase unbalance of three-phase as supply," ," *Journal of Scientific and Industrial Research*, Vol. 68, Jul. 2009, pp. 597-604.

[11] Copper for busbars, *Copper development association*, 1996, Pub. 22, sec. 6

[12] Petr M, Jiří M, Martin K & Miloš O, "Power Line Cable Transfer Function For Modeling Of Power Line Communication System," *Journal of Electrical Engineering*, Vol. 62, No. 2, 2011, pp. 104-108.

[13] A. Nazem & M. R. Arshad, "Combined Frequency and Amplitude Modulation in Power Line Communication (FAMPLC) for ROV control and monitoring," in *proceeding of 3rd International Conference on Underwater System Technology: Theory and Applications,* 2010, pp. 77-81.

[14] Introduction to Electronic circuit design, Richard R. Spencer, Mohammed S. Ghausi, Prentice Hall, 2003. pp. 1-15.

[15] Summerson S. R., "Equivalent Circuits and Transfer Functions," *technical report of the dept. of Electrical engineering, Rice university* 2009.

[16] S. Galli, T. Banwell, "A Novel Approach to the Modeling of the Indoor Power Line Channel," *Part II: Transfer Function and Its Properties, IEEE Transaction on Power delivery,* Vol. 20, No. 3, 2005. pp. 1869-1878. CrossRef

[17] Y. Liu, H. Hong, and A. Q. Huang, "Real-Time Calculation of Switching Angles Minimizing THD for Multilevel Inverters With Step Modulation," *IEEE Transaction on Industrial Electronics*, VOL. 56, NO. 2, 2009, pp. 285-293. CrossRef

[18] A. Nazem & M. R. Arshad, "Real Time Distant Communication Using Frequency And Amplitude Combined Modulations In Single Source Power Line (FAMPLC)," *International Conference on Advances in Electrical and Electronics Engineering*, 2011, pp.330-335.